AUTOMATED IDENTIFICATION OF RELATIVELY PERMANENT PIGMENTED OR VASCULAR SKIN MARKS (RPPVSM)

[1]Arfika Nurhudatiana, IEEE Student Member, [1]Adams Wai-Kin Kong, IEEE Member, [2]Lisa Altieri, and [2]Noah Craft

[1]School of Computer Engineering, Nanyang Technological University, Block N4, Nanyang Avenue, Singapore, 639798; [2]Los Angeles Biomedical Research Institute at Harbor-UCLA Medical Center, 1124 West Carson St. HH-207, Torrance, CA 90502 USA

ABSTRACT

In cases of child pornography and child sexual abuse, criminals are usually careful to hide or cover their faces and tattoos, thus making identification difficult. However, naturally occurring skin marks can be observed in close-up views of their back, chest, or thighs, which are usually present in evidence images. Recently, a group of skin marks named Relatively Permanent Pigmented or Vascular Skin Marks (RPPVSM) was proposed as a biometric trait for identification. Manual RPPVSM identification can be tiring and time consuming. We propose in this paper an automated RPPVSM identification system, which is composed of RPPVSM detection and matching algorithms. Three learning-based detection algorithms were developed to automatically detect RPPVSMs in color images. To evaluate these algorithms, experiments were performed on a database containing 216 back torso images from 118 subjects. The results show that high identification accuracy can be achieved and that the proposed RPPVSM identification system has high potential for forensic investigation.

Index Terms **—** Skin marks, detection, matching, identification, forensics

1. INTRODUCTION

Identification can be a challenging task in some forensic cases. For example, in cases of child pornography and child sexual abuse, criminals are usually careful to hide or cover their faces and tattoos. However, evidence images often show close-up views of their back, chest, or thighs, where naturally occurring skin marks can be observed. Recently, a group of skin marks named Relatively Permanent Pigmented or Vascular Skin Marks (RPPVSM), which can be found on almost any part of the human body, was proposed as a biometric trait for forensic identification [1]. RPPVSMs include but are not limited to nevi, lentigines, cherry hemangiomas, and seborrheic keratoses. Nevi (melanocytic nevi) or moles are sharply-circumscribed and chronic lesions of the skin. Their color ranges from skin-colored to black and their shapes are either elliptical or circular. They occur when melanocytes, which are pigment-producing cells, do not uniformly spread throughout the skin but instead grow in clusters. Lentigines, or lentigos, are flat pigmented spots on the skin, which can be irregular in shape. Lentigines occur as a result of an increase in the number of melanocytes with a linear spread. Cherry hemangiomas are red-colored papules containing an abnormal proliferation of blood vessels. These angiomas are benign cell growths derived from the cells of the vascular or lymphatic vessel walls (epithelium) or from cells of the tissues surrounding these vessels. Seborrheic keratoses are oval and slightly raised lesions, which occur due to proliferations of keratinocytes. Sometimes, the proliferating keratinocytes trigger the activation of neighboring melanocytes, resulting in pigmented seborrheic keratoses [2]-[3].

Manual RPPVSM identification can be tiring and time consuming. According to a statistical study in [1], Caucasians tend to have many RPPVSMs. Some Caucasians may have more than one hundred RPPVSMs on their back torsos. We propose in this paper an automated RPPVSM identification system for automatically detecting RPPVSMs in color images and matching RPPVSM patterns stored in a database. To the best of our knowledge, this is the first work on automated personal identification using non-facial skin marks.

Skin marks are utilized in face recognition systems as additional means of distinctiveness (e.g., in twin identification) or as an alternative biometric trait when face recognition fails (e.g., due to occlusions). Pierrard and Vetter [4] detected facial nevi by using a template matching technique based on a Laplacian of Gaussian (LoG) filter and classified them by using a saliency measure with contrast as a feature. Park and Jain [5] employed ten types of skin marks — freckles, moles, scars, pockmarks, acnes, whitening, dark skin, abrasions, wrinkles, and others, for improving the accuracy of their face matching system. They used a Laplacian of Gaussian (LoG) filter to detect potential facial skin marks and a rule-based classifier based on contrast and morphology features to classify them. Srinivas et al. [6] used eleven types of skin marks to distinguish

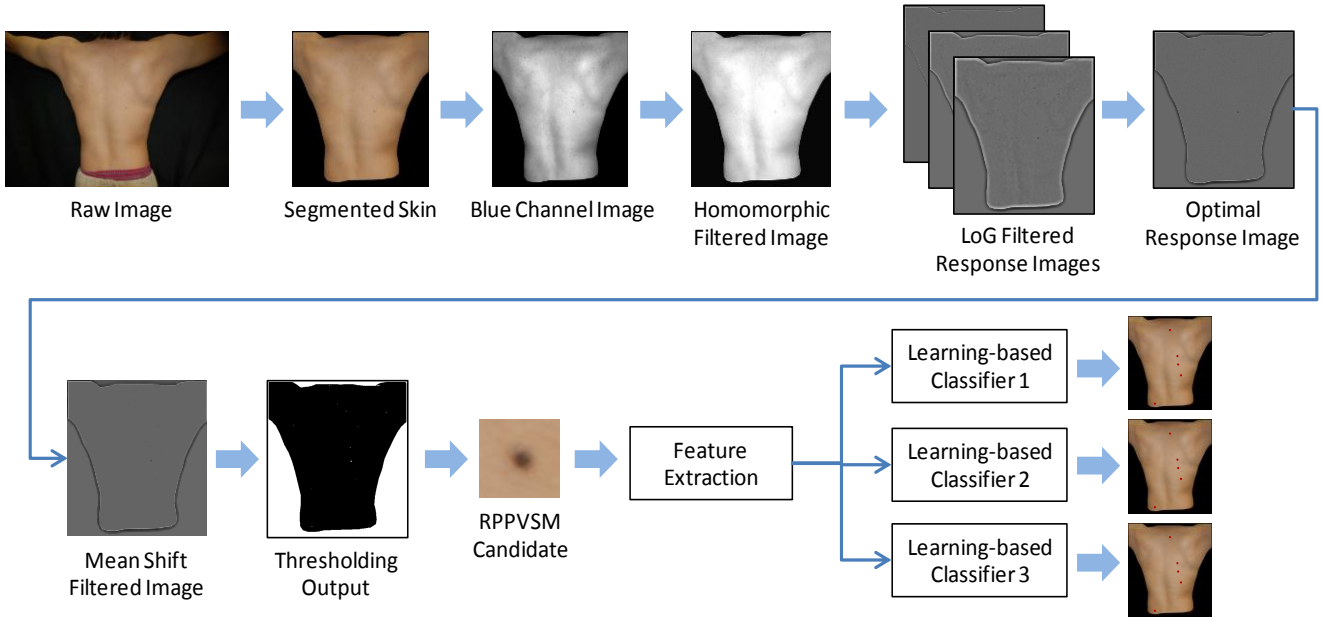

Fig. 1. A schematic diagram of the proposed detection algorithms

between identical twins. They were detected by a fast radial symmetry transform and a Gaussian pyramid. The skin marks employed in these face recognition systems vary from temporary marks (e.g., acnes, freckles) to permanent marks and were not classified by medical experts of the skin. RPPVSMs are medically well-defined and thus have more specific descriptions compared to these facial skin marks. It should be mentioned that RPPVSMs are stable for six months or longer and although they can be surgically removed, RPPVSMs are generally considered "relatively permanent".

In addition to personal identification, automated skin mark detection is also employed in melanoma diagnosis. Cho et al. [7] used Difference of Gaussian (DoG) filters followed by Support Vector Machine (SVM) to locate nevi on arms and back torsos. Lee et al. [8] used meanshift clustering, region growing, and a rule-based approach to locate nevi on back torsos. Matching algorithms were not offered in [7]-[8] since the proposed systems were intended for diagnosis.

The rest of this paper is organized as follows. Section 2 presents the proposed RPPVSM detection algorithms. Section 3 presents the matching algorithm. Section 4 reports experimental results. Section 5 provides conclusion of this paper.

2. RPPVSM DETECTION ALGORITHMS

The proposed RPPVSM detection algorithms are comprised of four steps: 1) preprocessing, 2) RPPVSM candidate detection, 3) feature extraction, and 4) classification. The schematic diagram of the proposed detection algorithms is given in Fig. 1. In the preprocessing stage, the skin region is manually segmented from the raw color image. Then, the blue channel in the RGB color space is extracted from the segmented skin image. The blue channel contains the richest information for RPPVSM detection since these skin marks, located on the surface of the skin, are most sensitive to the wavelengths in the blue channel compared to wavelengths in the other channels, which penetrate into the deeper layers of the skin. The blue channel is then converted into a grayscale image by adjusting the intensity values such that they range from 0 to 1. The image is further processed by homomorphic filtering [9]. A homomorphic filter normalizes the brightness across an image and increases the contrast by separating illumination field from the reflectance field.

After preprocessing, LoG kernels with $\sigma = 0.5$ and 5 different scales (filter sizes = 10x10, 20x20, 30x30, 40x40, and 50x50) are used to detect RPPVSM candidates of different sizes. An optimal response image IM_{opt} defined as

$$IM_{opt}(x, y) = \max_{s} IM_{LoG_s}(x, y), \quad (1)$$

where IM_{LoG_s} is the response image from the LoG filter with scale s, is obtained. The optimal response image is then smoothed using the mean shift algorithm [10]. Mean shift is an edge-preserving smoothing algorithm. It iteratively calculates a new mean in a given set of pixels until the mean stops changing. The clusters are then represented by these mean values. To segment the RPPVSMs, the smoothed image undergoes a binarization process through the following thresholding operation:

$$L(x,y) = \begin{cases} 1 & \text{if } t_1 \le I(x, y) \le t_2 \\ 0 & \text{otherwise,} \end{cases} \quad (2)$$

where $L(x,y)$ is a binary label of a pixel at (x,y) coordinate, I is a grayscale intensity image after the mean shift filtering, and t_1 and t_2 are minimum and maximum thresholds,

respectively. The pixel intensity values of RPPVSMs are lower than the surrounding skin. We tried a range of values for t_1 and t_2 and selected the values which gave the closest results to manual markings by dermatologists. In the experiments, t_1 and t_2 were set respectively to 0.01 and 0.42. Finally, a morphological close operation is applied to obtain a smooth segmentation output.

The output of the RPPVSM candidate detection may still include non-RPPVSMs, such as scars, acne lesions, or hairs. To reject these non-RPPVSMs, a classification scheme to differentiate between these two groups is required. Five types of features which include contrast, shape, size, texture, and color are considered for classification. For contrast measurement, two bounding boxes, BB_1 and BB_2, are used (see Fig. 2). The first bounding box, BB_1, encloses the region of the detected RPPVSM candidate, while the second bounding box, BB_2, encloses the neighboring area of BB_1 by p distance pixels. We set $p = 2$ in this study. Contrast is described using two parameters c_1 and c_2:

$$c_1 = \frac{1}{N}\sum_{i\in BB_1} I_i, c_2 = \frac{1}{M}\sum_{j\in BB_2\setminus BB_1} I_j, \quad (3)$$

where N is the number of pixels in BB_1, M is the number of pixels in $BB_2\setminus BB_1$, and I_i and I_j are the intensity values of the i^{th} and j^{th} pixel, respectively. Contrast is measured on the contrast-enhanced image produced by homomorphic filtering. Since RPPVSMs generally are circular or elliptical, their shapes can be described using three elliptical properties: 1) eccentricity, 2) major axis length, and 3) minor axis length. Eccentricity is a measure of circularity in an elliptical object. Eccentricity of value 0 indicates a circle while eccentricity of value 1 indicates a line segment. Size is defined as the number of connected pixels which are labeled as RPPVSM. Texture information is obtained from the histogram of the rotationally invariant uniform Local Binary Pattern [11]. Color parameters are the minimum, maximum, and average normalized intensity values of the R, G, and B channels respectively. Finally, each sample is represented by a 25-dimensional feature vector, which is the classifier input.

Three learning-based classifiers, which include a binary decision tree, a three-layered feed-forward neural network, and a SVM, were implemented to separate between RPPVSMs and non-RPPVSMs in the candidate set. The decision tree used Gini's diversity index as the split criterion. The SVM was trained with a linear kernel function. The neural network had 10 neurons in the hidden layer and tan-sigmoid transfer functions in the hidden and output layers, and was trained using the scaled conjugate gradient back-propagation algorithm. All these classifiers were trained using the same dataset, which will be described in Section 4.

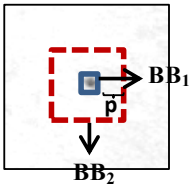

Fig. 2. Two bounding boxes BB_1 and BB_2 for measuring the contrast feature

3. RPPVSM MATCHING

RPPVSM matching involves registration and matching score calculation. Registration is the process of aligning two RPPVSM patterns; one pattern is an input (e.g., from evidence image) and the other one is a template (e.g., from a database). We use the shape of back torso for registration. First, the boundary of back torso is detected by applying the Roberts edge detector [12] to the skin-segmented image. The detected boundary pixels are subsequently down-sampled. The remaining boundary points and the detected RPPVSM points together are used as input to the matching algorithm. The non-rigid Coherent Point Drift (CPD) algorithm is employed to perform the registration [13]. Since the number of boundary points is much larger than the number of detected RPPVSMs, the alignment is largely influenced by the shape of the back torso. After the two back torsos from the template and the input images are aligned, matching score is calculated. A k-Nearest Neighbor algorithm with k = 1 is used to search for candidate correspondences. A correspondence between two RPPVSMs, where one is from an input and the other one is from a template, is established if $d \le r_0$, where d is the distance between the two RPPVSMs and r_0 is a tolerance distance parameter. Finally, the matching score, defined as $2c/(m+n)$, where c is the number of correspondences, m is the number of RPPVSMs in the template pattern, and n is the number of RPPVSMs in the input pattern, is calculated. Fig. 3 illustrates the steps to generate the points used in the RPPVSM matching.

4. EXPERIMENTAL RESULTS

Our database contains 216 color images from 118 Caucasian, Asian, and Latino subjects. There are 20 subjects with a single image and 98 subjects with two images. The images were divided into a training dataset (20 single images) and a testing dataset (196 images from the 98

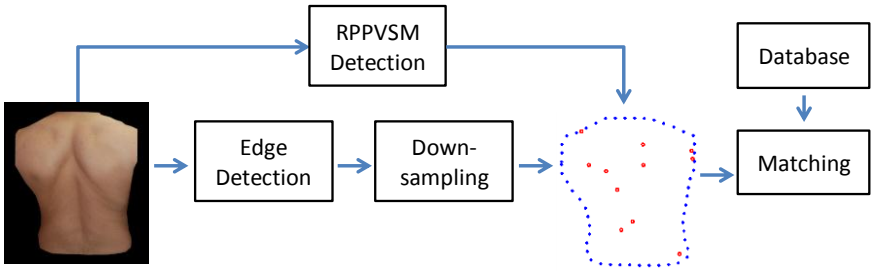

Fig. 3. Steps to generate the points used in the RPPVSM matching

subjects) with no overlap between the two sets. The RPPVSMs in the training dataset were manually labeled by three dermatologists, resulting in 234 samples of RPPVSMs. Samples of non-RPPVSMs were obtained by applying the proposed RPPVSM candidate detection algorithm to the 20 training images. The detected RPPVSM candidates which were not marked as RPPVSMs were labeled as non-RPPVSMs. Finally, we obtained 234 RPPVSMs and 628 non-RPPVSMs from the training dataset. The matching parameter r_0 was determined from

$$Pr\left(3 \times major\ axis\ length\ of\ a\ RPPVSM \le r_0\right) \ge t, \qquad (4)$$

where t is a statistical threshold. From the 234 RPPVSM samples in the training dataset, we obtained $r_0 = 23$ pixels for $t = 95\%$. As for the testing dataset, some images of the same subject were taken in two different sessions with different lighting conditions while the rest were taken in different poses. RPPVSMs in the testing dataset were completely detected automatically.

To evaluate the proposed automated RPPVSM detection algorithms, we matched each image in the testing dataset with the remaining 195 images. The probability of randomly matching the input RPPVSM patterns with the corresponding one is 1/195. The identification accuracies of the proposed algorithms are given in Fig. 4. Rank-10% identification accuracy refers to the percentage of input RPPVSM patterns whose corresponding template RPPVSM patterns can be found in the top 10% patterns returned by the algorithm.

The SVM gave the highest rank-10% identification accuracy of 96.43% and achieved 100% identification at rank-30%. The neural network gave rank-10% identification accuracy of 91.84%, followed by the decision tree with rank-10% identification accuracy of 79.59%. Additionally, we also observed that the detection output of the SVM classifier is the closest to the dermatologists' markings compared to the other classifiers. These results indicate that the proposed algorithms have high potential to be applied in forensic cases.

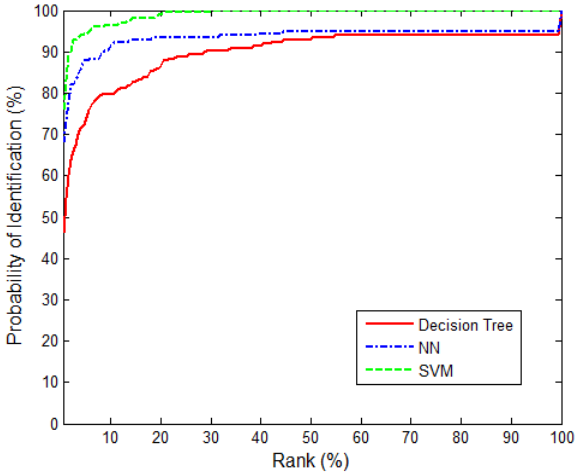

Fig. 4. Identification accuracy of the proposed algorithms

Although the proposed RPPVSM identification algorithms work well for most images, they failed in some cases. For some images, NN and decision tree could not detect any RPPVSMs and therefore, the corresponding matching scores were always zero. Fig. 5a shows an image of a subject with 10 detected RPPVSMs. However, these RPPVSMs could not be detected from the corresponding image of the same subject because the second image was out-of-focus (see Fig. 5b).

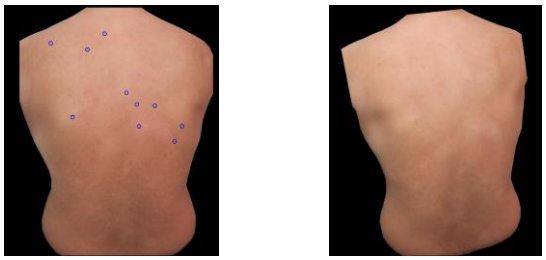

(a) (b)

Fig. 5. A sample scenario when identification failed. (a) 10 RPPVSMs were detected from an image of a subject, (b) no RPPVSMs were detected from another image of the same subject in (a) when the image is out-of-focus.

5. CONCLUSION

We present in this paper the first work on automated Relatively Permanent Pigmented or Vascular Skin Marks (RPPVSM) identification. Although several facial skin mark identification methods are available, the work presented here focuses on a specific group of medically identifiable skin marks named RPPVSM. RPPVSMs are not specific to the face and can be recognized on almost every part of the human body. In addition to the contrast and shape features, which are commonly used in the skin mark detection methods, texture, area, and color were also included. We implemented three different types of learning-based classifiers and the results show that the proposed feature set is effective for RPPVSM classification. Furthermore, the matching results indicate that the proposed RPPVSM identification system has the potential for application in forensic cases. For future work, we will include more images with varying poses, view angles, and lighting conditions since evidence images are usually captured in uncontrolled environment settings. We also plan to improve the RPPVSM detection and matching algorithms.

6. ACKNOWLEDGMENTS

We would like to thank the Singapore Prison Service and the Singapore Police Force for their legal and forensic discussions. This work is partially supported by the Ministry of Education, Singapore through Academic Research Fund Tier 2, MOE2012-T2-1-024.

7. REFERENCES

[1] A. Nurhudatiana, A.W.K. Kong, K. Matinpour, S.-Y. Cho, and N. Craft, "Fundamental Statistics of Relatively Permanent Pigmented or Vascular Skin Marks for Criminal and Victim Identification," in *Proc. IJCB*, pp. 1-6, Washington DC, 2011.

[2] J.M. Grichnik, A.R. Rhodes, and A.J. Sober, *Fitzpatrick's Dermatology in General Medicine,* 7th ed., McGraw-Hill, 2008.

[3] W. James, T. Berger, and D. Elston, *Andrew's Diseases of the Skin: Clinical Dermatology,* 10th ed., Saunders, 2005.

[4] J.S. Pierrard and T. Vetter, "Skin Detail Analysis for Face Recognition," in *Proc. CVPR*, pp. 1-8, Minneapolis, 2007.

[5] U. Park and A.K. Jain, "Face Matching and Retrieval Using Soft Biometrics," *IEEE Trans. Information Forensics and Security*, vol. 5, no. 3, pp. 406-415, 2010.

[6] N. Srinivas, G. Aggarwal, P.J. Flynn, and R.W.V. Bruegge, "Analysis of Facial Marks to Distinguish Between Identical Twins," *IEEE Trans. Information Forensics and Security*, vol. 7, no. 5, pp. 1536-1550, 2012.

[7] T.S. Cho, W.T. Freeman, and H. Tsao, "A Reliable Skin Mole Localization Scheme," in *Proc. ICCV*, pp. 1-8, Rio de Janeiro, 2007.

[8] T.K. Lee, M.S. Atkins, M.A. King, S. Lau, and D.I. McLean, "Counting Moles Automatically From Back Images," *IEEE Trans. Biomedical Engineering*, vol. 52, no. 11, pp. 1966-1969, 2005.

[9] V. Madisetti and D.B. Williams, *Digital Signal Processing Handbook*, CRC Press, 1997.

[10] D. Comaniciu and P. Meer, "Mean Shift: A Robust Approach Toward Feature Space Analysis," *IEEE Trans. Pattern Analysis and Machine Intelligence*, vol. 24, no. 5, pp. 603-619, 2002.

[11] T. Ojala, M. Pietikäinen, and T. Mäenpää, "Gray Scale and Rotation Invariant Texture Classification with Local Binary Patterns," in *Proc. ECCV*, pp. 404-420, Dublin, 2000.

[12] L.G. Roberts, "Machine Perception of Three-Dimensional Solids," in *Optical and Electro-Optical Information Processing* (J. Tippett, D. Berkowitz, L. Clapp, C. Koester, A. Vanderburgh, Eds.), MIT Press, pp. 149-197, 1965.

[13] A. Myronenko and X. Song, "Point Set Registration: Coherent Point Drift," *IEEE Trans. Pattern Analysis and Machine Intelligence*, vol. 32, no.12, pp. 2262-2275, 2010.